Postprint

Towards the Development of a Novel Upper-Body Pneumatic Humanoid: Design and Implementation

George Andrikopoulos, *Member, IEEE*, George Nikolakopoulos, *Member, IEEE*,
Dariusz Kominiak, Åsa Unander-Scharin

Abstract— In this article, the conceptual design of a 14 Degree-of-Freedom (DoF) upper-body pneumatic humanoid is presented. The movement capabilities of this novel robotic setup are achieved via Pneumatic Artificial Muscles (PAMs), a form of actuation possessing crucial attributes for the development of biologically-inspired robots. To evaluate the feasibility of the humanoid's design properties, a 5-DoF robotic arm is developed and experimentally tested, while being studied from the scope of implementing a robotic structure capable of producing smooth and human-like motion responses, while maintaining the inherent compliance provided by the PAM technology.

I. INTRODUCTION

During the past few years, the use of inherently compliant materials, characterized by flexibility and biomimetic attributes has been the interest of researchers and manufacturers. Specifically, there has been a large research attempt in improving the design of humanoid robots and produce setups with motion capabilities inspired by the smoothness, accuracy and compliance that characterize the human motion [1], [2]. Muscle emulation, is still one of the biggest challenges, where the overall goal is to create an actuator that combines the power, accuracy and durability of mechanical drives, with the safety, controllable compliance and efficiency of natural muscles [3] by macroscopically emulating some of its inherent functionality.

In this article, the conceptual design of a novel upper-body humanoid will be presented, which is considered as the mandatory infrastructure for enabling future interactive applications driven by smooth, fast and accurate upper-body movements. Specifically, the proposed upper-body robot is designed to reproduce the following human-inspired movements: a) wrist radial/ulnar deviation, b) elbow flexion/extension, c) shoulder flexion/extension, d) shoulder abduction/adduction, e) shoulder medial/lateral rotation, f) neck flexion/extension, g) neck lateral bending, h) neck bending and i) lower back flexion/extension.

For actuation purposes, the robotic humanoid utilizes Pneumatic Artificial Muscles (PAMs) in order to achieve the 14 Degree-of-Freedom (DoF) movements performed via its biologically-inspired arms, neck and lower back [4]. The

PAM is a tube–like pneumatic actuator that is characterized by a decrease in the actuating length when pressurized, while possessing similar properties with those of the organic muscle, combined with several advantages as the ability to provide high power outputs, with relatively light weights and inherent compliance. These characteristics are turning the PAM into a promising actuator choice in anthropomatic technologies, since it meets the need for safety, simplicity and lightness that human–robot interaction requires, thus justifying its expanding utilization in medical and biorobotic applications [5].

The main contribution of this article stems from the design of a novel robotic humanoid via the utilization of PAM technology, as well as the feasibility study performed through the development and experimental evaluation of a PAM-actuated pneumatic arm. In the proposed design, which acts as an alternative mechanical solution to the existing approaches in the related literature [6]–[11], the reduced-DoF mechanism is considered as a basic motion problem, however, the conceptual design from an engineering point of view and without losing generalization, can form the basis for its expansion in developing a compliant, safe and motion accurate full-body humanoid.

The rest of the article is structured as follows. In Section II, the 14-DoF upper-body pneumatic humanoid is presented in detail from a conceptual point of view, while presenting the design specifics of the utilized motion strategy for undertaking the humanoid's motion capabilities. Section III provides an overview of the various components utilized for the performed feasibility study via the development of a 5-DoF humanoid arm and Section IV presents a experimental evaluation of the arm's capabilities in reproducing human-like movements. Finally, a summary of the main contributions of this work are presented in Section V.

II. CONCEPTUALIZATION OF AN UPPER-BODY HUMANOID

A. Conceptual Design

The overall design properties of the proposed upper-body pneumatic humanoid are depicted in Fig. 1. The biologically-inspired concept is formed on the basis of the endoskeleton dimensions of an adult human, while following a muscle-tendon-based approach for the generation of the robot's movements. This design strategy leads to a reduced-DoF alternative of the following movements: a) wrist (radial/ulnar deviation), b) elbow (flexion/extension), c) shoulder (flexion/extension, medial/lateral rotation, abduction/adduction), d) neck (rotation) and e) lower back (flexion/extension). Considering the two upper-limb approach, this design leads to a total of 14-DoFs.
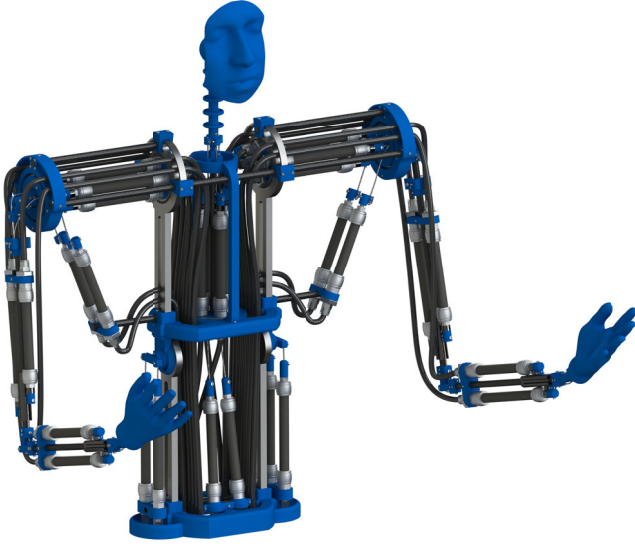
Figure 1. Conceptual design of the proposed upper-body pneumatic humanoid.

The number and placement of the PAMs for the enablement of the humanoid's DoFs has been properly selected so as to simplify the complexity of the various movement scenarios by taking advantage of an antagonistic PAM movement strategy, where PAMs are working antagonistically between pairs [12]. The antagonistic PAM pairs utilized in the proposed structure are depicted in Fig. 2(a), accompanied by color-matched information to the respective movements.

When considering the use of PAMs for the actuation of a biomimetic design, the available contraction and its direct connection to the produced contractile force play a major role on the joint design strategy. It has to be noted that the PAM technology provides a maximum of 30% permissible stroke, which when compared to the 50-70% of the biological muscle [13], creates challenges in producing similar motion ranges for given joint dimensions. This challenge is also addressed by the fact that the forces exerted on the PAMs during movement have a direct impact on its permissible contraction [14]. Taking all these properties into consideration, the design approach of the proposed upper-body humanoid follows a trade-off between joint angle and torque by incorporating a biomimetic muscle-tendon strategy. The tendon-like strings utilized to transfer the PAM linear motion to the joints, as well as the properties of the utilized joints, are presented in Fig. 2(b), where θ denotes the angular motion of the i-th joint for $i = 1,…,14$. Note that joints $i = 1,…,5$ and $i = 6,…10$ correspond to the PAM pairs used in the two symmetrical shoulder-arm mechanisms, respectively, while $i = 11,…,13$ correspond to the PAM pairs of the neck and $i = 14$ to the pair responsible for the lower back movement. In addition, the design involves the use of bearing-based revolute joints for the upper body movements, except for the neck flexion/extension and lateral bending movements, where a spherical joint is appropriately attached into the spine-inspired formation.

Details of the tendon mechanisms utilized in the wrist, elbow and shoulder of are presented in Fig. 3, which shows the main design strategy for converting the PAMs' linear

(a)

(b)

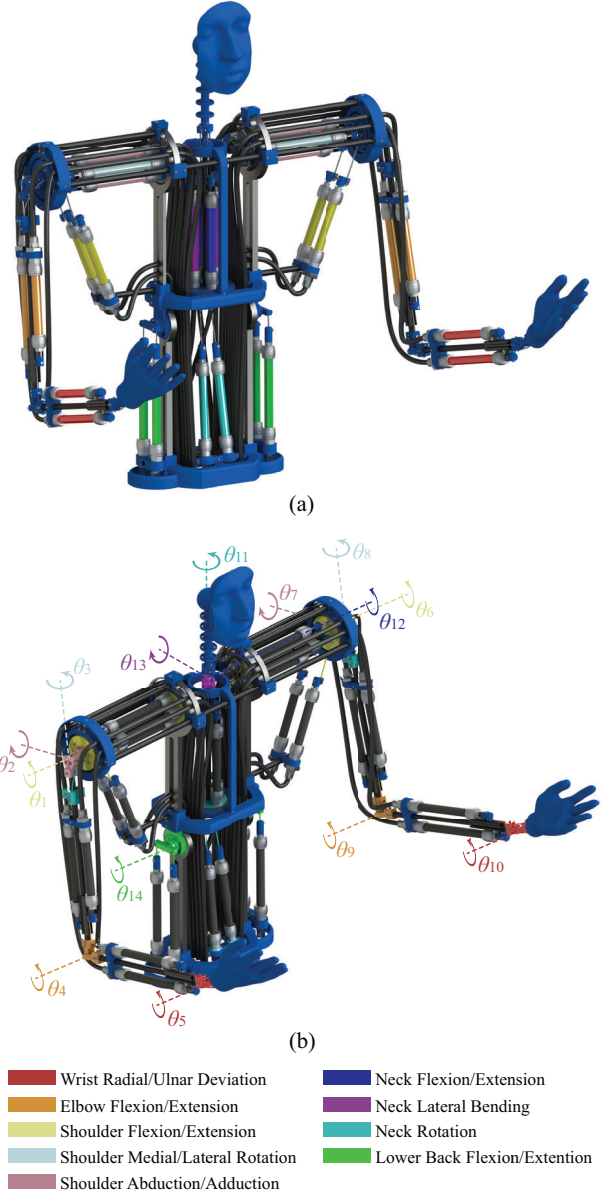|			
▮ Wrist Radial/Ulnar Deviation		▮ Neck Flexion/Extension	
▮ Elbow Flexion/Extension		▮ Neck Lateral Bending	
▮ Shoulder Flexion/Extension		▮ Neck Rotation	
▮ Shoulder Medial/Lateral Rotation		▮ Lower Back Flexion/Extention	
▮ Shoulder Abduction/Adduction			

Figure 2. Color-highlighted (a) antagonistical pairs of PAMs, (b) revolute/spherical joints and tendons accompanied by the respective generated movements.

displacement to angular movement. All tendons are properly attached to the PAMs' end cap parts and to the respective point of rotation, where appropriate inlets on the endoskeleton structure are utilized to guide the tendons' movement and ensure smoothness and efficiency.

The concept followed in achieving the shoulder's 3-DoFs involved the use of mechanically independent rotation points via appropriately designed endoskeletal parts, as shown in Fig. 3(c). Challenging motion patterns as the shoulder's medial/lateral rotation are addressed via the use of eccentric connections of the tendons to the bearing-based joints, thus forcing a planar motion transfer during the activation of the respective PAM pair and the successful rotational movement of the joint. This strategy enabled the PAMs involved in these movements to be placed on the shoulder endoskeletal area, rather than the space around the back and abdomen,
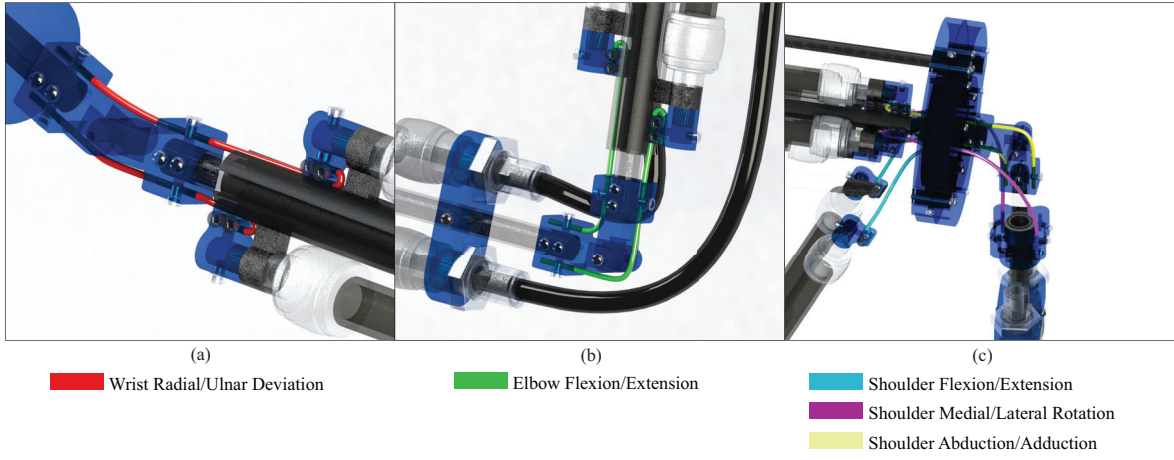
Figure 3. Details of the tendon-based motion mechanism for the (a) wrist, (b) elbow and (c) shoulder joints.

thus providing a novel design alternative. A basic advantage of this strategy is the mechanical decoupling of the shoulder's medial/lateral rotation from the flexion/extension and abduction/adduction, since the two latter ones can now be performed independently of the shoulder rotation state.

B. Antagonistic Motion Strategy

In order to take advantage of the full PAM stroke and thus, ensure the maximum provided range of motion for every DoF, the PAMs are initially inflated at a P_0 pressure which corresponds to the half of their maximum permissible stroke, before being connected to their respective tendons. With that in mind, the antagonistic movement strategy is formulated in (1), where $P_{i,j}$ defines the pressure values utilized in every antagonistic pair of PAMs, identified as $j = 1,2$, for the undertaking of the $i = 1,\dots,14$ joint movements described in the previous Subsection, while $P_{i,0}$ denotes the initial pressure of the i-th PAM pair. This strategy has the advantage of utilizing one manipulated pressure variable ΔP_i that is being respectively added and subtracted from the antagonistic PAM pair and depending on its sign causes the desired motion pattern.

$$P_{i,j} = P_{i,0} \pm \Delta P_i \text{ for } \begin{cases} i=1,6 \Rightarrow \begin{cases} \text{Wrist Radial } (\Delta P_i > 0) \\ \text{Ulnar Deviation } (\Delta P_i < 0) \end{cases} \\ i=2,7 \Rightarrow \begin{cases} \text{Elbow Flexion } (\Delta P_i > 0) \\ \text{Elvow Extension } (\Delta P_i < 0) \end{cases} \\ i=3,8 \Rightarrow \begin{cases} \text{Shoulder Flexion } (\Delta P_i > 0) \\ \text{Shoulder Extension } (\Delta P_i < 0) \end{cases} \\ i=4,9 \Rightarrow \begin{cases} \text{Shoulder Medial Rotation } (\Delta P_i > 0) \\ \text{Shoulder Lateral Rotation } (\Delta P_i < 0) \end{cases} \\ i=5,10 \Rightarrow \begin{cases} \text{Shoulder Abduction } (\Delta P_i > 0) \\ \text{Shoulder Adduction } (\Delta P_i < 0) \end{cases} \\ i=11 \Rightarrow \text{Neck Right Rotation } (\Delta P_i > 0, \Delta P_i < 0) \\ i=12 \Rightarrow \begin{cases} \text{Neck Flexion } (\Delta P_i > 0) \\ \text{Neck Extension } (\Delta P_i < 0) \end{cases} \\ i=13 \Rightarrow \text{Neck Lateral Bending } (\Delta P_i > 0, \Delta P_i < 0) \\ i=14 \Rightarrow \begin{cases} \text{Lower Back Flexion } (\Delta P_i > 0) \\ \text{Lower Back Extention } (\Delta P_i < 0) \end{cases} \end{cases} \quad (1)$$

Based on the system's characteristics and the motion attributes, appropriate constraints are posed on the operating pressure, by setting minimum and maximum limits as specified in (2):

$$P_{\min} \leq P_{i,j} \leq P_{\max} \quad (2)$$

III. FEASIBILITY STUDY

A. Pneumatic Humanoid Arm Prototype

For the evaluation of the conceptual design described in the previous Section, a 5-DoF pneumatic humanoid arm was developed by following the mechanical strategies implemented in the proposed humanoid robot. The prototype version that was developed for this feasibility study is presented in Fig. 4, along with highlights of the basic components of its skeletal structure and actuation.
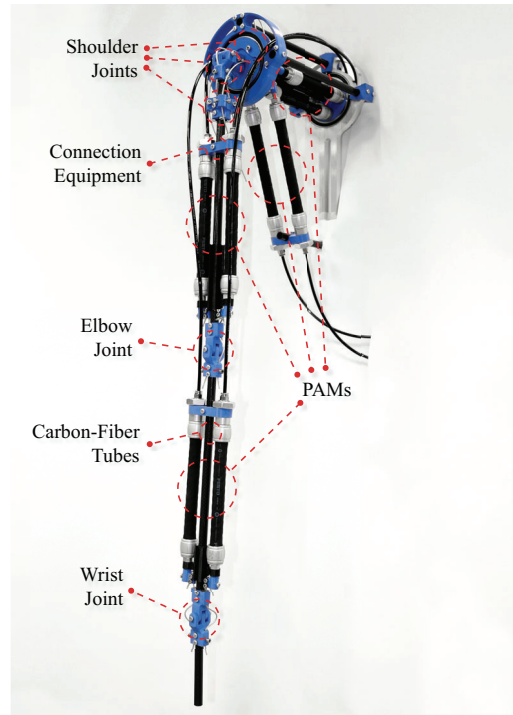

Figure 4. Pneumatic humanoid arm prototype.

Overall, ten FESTO Fluidic Muscles have been utilized for the reproduction of the 5-DoFs of the wrist, elbow and shoulder by following the conceptual design described in the previous Section. Specifically, six DMSP-10-120N-AM-CM with 10 mm internal nominal diameter and 120 mm nominal length are utilized for the wrist, elbow and shoulder flexion/extension movements, while four DMSP-10-100N-AM-CM with 10 mm internal nominal diameter and 100 mm nominal length are incorporated for the shoulder rotation and abduction/adduction movements. The nominal length of the PAMs has been appropriately selected by taking into consideration the dimension restrictions of the biomimetic design, which are ultimately posed by the human body. Moreover, the PAMs' placement upon the skeletal structure of the arm plays a crucial role to the robot's motion quality, since it acts as a trade-off between the acquired angular motion and the torque generated on the respective joints, considering the fact that the utilized PAMs can be operated between their permissible pressure range 0 – 8 bar.

In addition, low-weight materials have been utilized in the development of the skeletal structure In order to minimize the inertial effects of the arm's equipment during joint motion. Specifically, the skeleton consists of carbon-fiber tubes in order to provide increased durability, as shown in Fig. 4, while the various connection components and the joint parts have being 3D printed via PLA material. Also, steel wire has been selected for the role of the artificial tendons, while being equipped with plastic coating to decrease the friction phenomena during contact with the 3D-printed joints. Finally, metal bearings have been appropriately incorporated in the joint mechanisms for increased motion sensitivity and smoothness. The above selection of materials led to a robotic humanoid arm that weighs approximately 2 kg, of which 0.8 kg belong to the utilized PAMs. To the author's knowledge, this is one of the smallest documented weights in related bibliography regarding a 5-DoF human-size arm [1], [2].

B. Experimental Setup Components

Regarding additional setup components, ten FESTO VPPM-6F-L-1-F-0L10H-V1N-S1 proportional pressure regulators have been utilized to control and measure the pressure of the compressed air supplied into the PAMs. The utilized pressure sensors, which are integrated inside the aforementioned pressure regulators, provide a measurement accuracy of ±0.0035 bar. Moreover, a VICON motion capturing system consisted of twenty IR cameras has been utilized for the measurement and acquisition of angular and translational motion data of the humanoid arm prototype. The specific equipment ensures high-accuracy measurements, as it provides translation accuracy of approximately 0.04 mm and a respective angular accuracy of 0.02 degrees. Finally, the control of the setup's operation, as well as the data acquisition, have been achieved via a USB-1608G and a USB-3100 data acquisition cards supplied by Measurement Computing, while the setup's programming software has been developed in National Instruments LabVIEW.

IV. PRELIMINARY EXPERIMENTAL EVALUATION

In this section, experimental studies are presented to test the pneumatic humanoid arm's 5-DoFs, as well as to evaluate
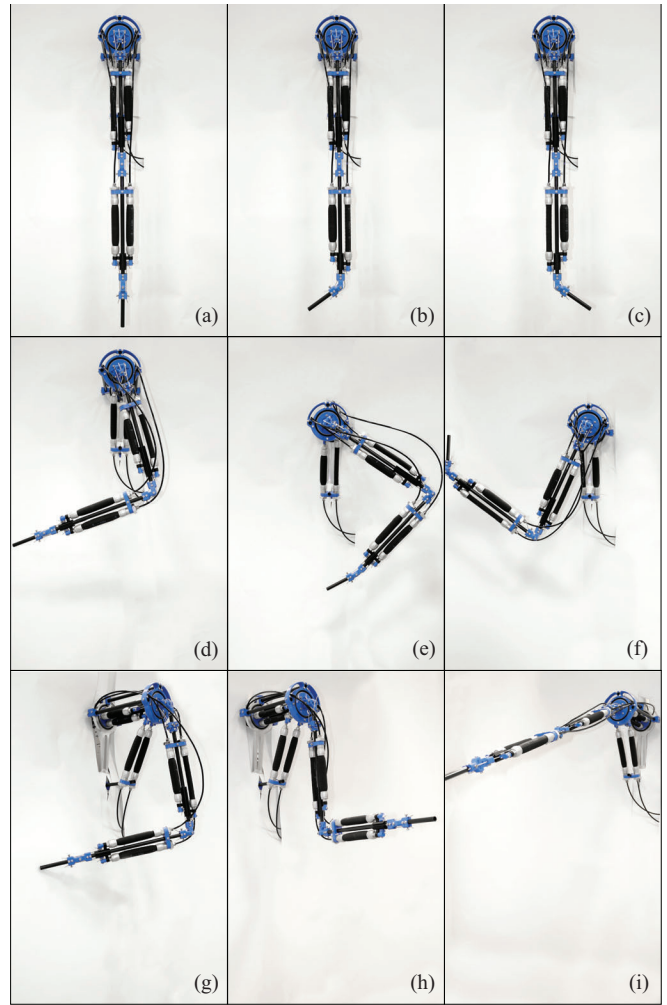

Figure 5. Experimental details of the various motion scenarios highlighting the humanoid arm's (a) idle state, (b) wrist radial deviation, (c) wrist ulnar deviation, (d) elbow flexion, (e) shoulder extension, (f) shoulder flexion, (g) shoulder medial rotation, (h) shoulder lateral rotation and (i) shoulder abduction motion capabilities.

its performance in reproducing human-like movements through its biomimetical wrist, elbow and shoulder. Specifically, extensive experimental trials concerning open-loop responses have been performed in order to test all possible movement patterns of the humanoid arm, while Fig. 5 presents photographs of the setup, which have been taken throughout these experimental sequences.

The translational and angular data of every joint have been recorded via the motion capturing system, as graphically presented in Fig. 6, thus providing an accurate measurement of the maximum angular range of the arm's joints, which are presented in Table I, with respect to the idle state depicted in Fig. 5(a). Also presented in this Table are the initial pressures $P_{0,i}$, which are utilized for the joints idle state. It has to be noted that throughout the trials, all pressure signals, which have been calculated via (1) via the appropriate change of the pressure element ΔP_i, were constrained to the PAM's permissible range $0 \leq P_{i,j} \leq 8$ bar.

In order to mimic the human elbow's inability to perform bi-directional movements, the maximum range regarding the elbows extension is considered as the idle state (Fig. 5(a)),
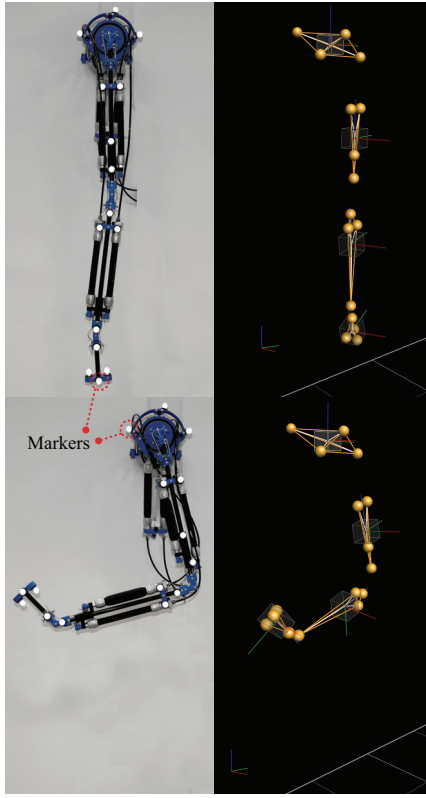
Figure 6. The pneumatic arm equipped with appropriately positioned markers during idle (top-left) and activated state (bottom-left). 3D reconstructed model through data acquisition via the VICON motion capturing system during idle (top-right) and activated state (bottom-right).

TABLE I. PNEUMATIC HUMANOID ARM'S RANGE OF MOTION

i	$P_{0,i}$ [bar]	Movement Type		Maximum Angle [deg]
1	3.78	Shoulder	Flexion	20.5
			Extension	31.2
2	3.55		Abduction	54.5
			Adduction	10.2
3	3.89		Medial Rotation	62.1
			Lateral Rotation	61.3
4	3.76	Elbow	Flexion	92.5
			Extension	0 (Idle)
5	3.70	Wrist	Radial Deviation	58.5
			Ulnar Deviation	59.3

which is noted in Table I as 0 degrees. In the same manner, the maximum shoulder adduction was constrained to approximately 10.2 degrees, in order to avoid the collision of the arm with the rest of the endoskeletal parts during this particular movement.

The acquired position data of the robotic arm's end effector during the repetition of the motion experiments for all joint combinations resulted in the reachable workspace of the proposed design, which is presented in Fig. 7 for the motion cases of: a) $i = 1,2$, b) $i = 1,..,3$, c) $i = 1,…,4$ and d) $i = 1,…,5$ active joints.

In addition, the open-loop angular responses of the pneumatic humanoid arm's elbow flexion/extension and wrist radial/ulnar deviation movements for sinusoidal
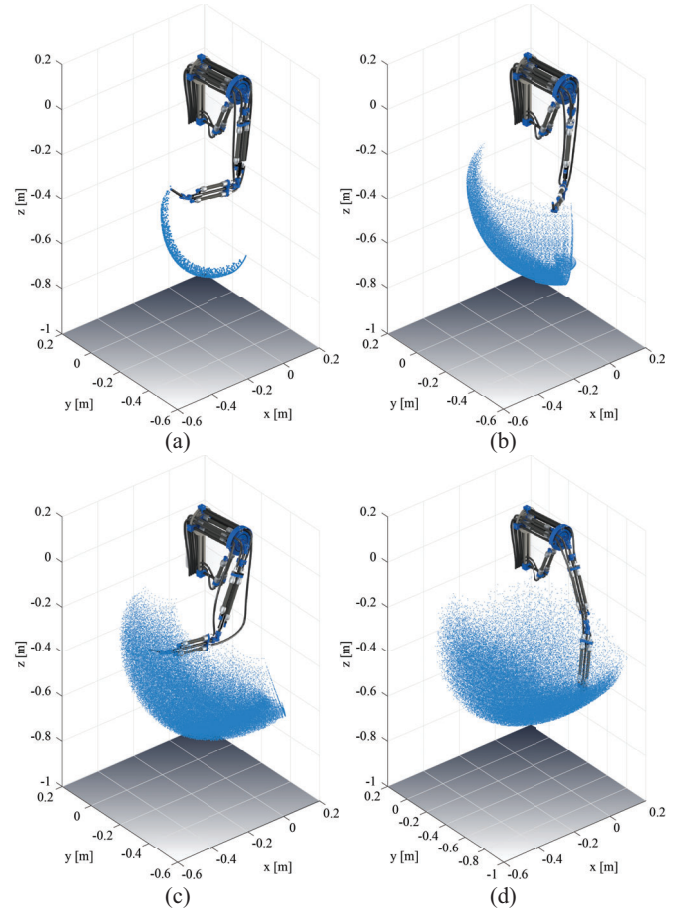

Figure 7. The pneumatic humanoid arm's experimentally acquired workspace regarding the movements produced via the activation of (a) $i = 1,2$, (b) $i = 1,..,3$, (c) $i = 1,…,4$ and (d) $i = 1,…,5$ active joints.
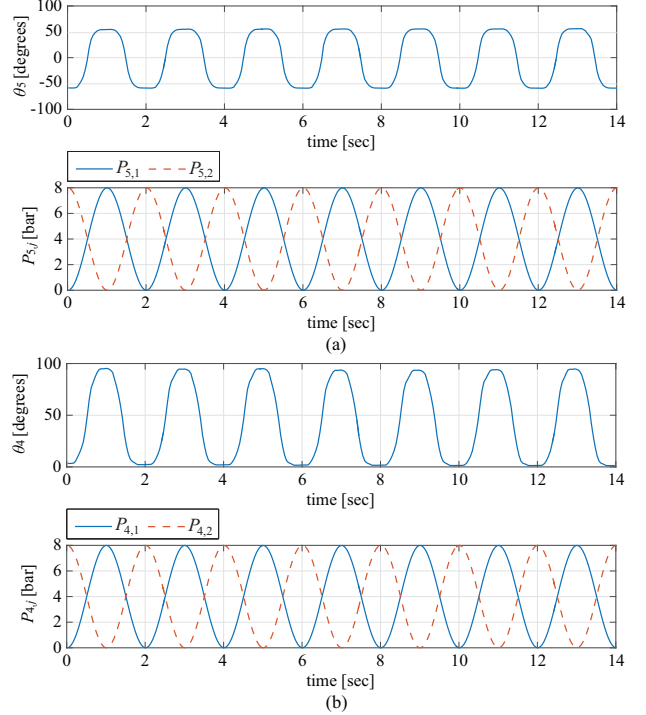

Figure 8. Open-loop angular responses of the arm's (a) wrist radial/ulnar deviation and (b) elbow flexion/extension movements for sinusoidal pressure signals.

pressure signals ranging between 0 and 8 bar (P_0 = 4 bar) at 0.5 Hz are presented in Fig. 8.

The presented results show that the proposed pneumatic humanoid arm manages to successfully perform the multiple DoF open-loop experiments, while producing human-like postures. The end-effector data presented in Fig. 7(d) for all 5-DoFs reveal the extensive workspace of the proposed design, which is characterized by sufficiently large ranges of motion, thus possessing the ability to reproduce various patterns. Moreover, the preliminary evaluation of the basic motion responses proves the structural capability of the proposed robotic structure in producing smooth and fast movements.

In overall, the experimental evaluation reveals that this novel endoskeletal design approach possesses the structural attributes necessary for biomimetic reproduction of the basic movements of the human arm and enables the expansion of this conceptual design towards the development of the proposed 14-DoF upper-body configuration.

V. CONCLUSIONS

In this article, the conceptual design of a 14 Degree-of-Freedom (DoF) upper-body pneumatic humanoid was presented in detail from a conceptual point of view, while giving additional insight to the design specifics of the utilized motion strategy for undertaking the humanoid's motion capabilities. For the evaluation of the conceptual design strategy, a feasibility study was performed via the development of a 5-DoF humanoid arm and the results of a preliminary experimental evaluation of the arm's motion capabilities were presented. The experimental evaluation revealed that this novel endoskeletal approach possesses the structural attributes necessary for biomimetic reproduction of the basic movements of the human arm, since it manages to successfully perform the multiple DoF open-loop experiments, while producing human-like postures and smooth motion responses.

The authors have to note that the presented research concerned the preliminary evaluation of the humanoid arm prototype, where the reduced-DoF approach was considered as a basic motion problem. Position control of the arm's joints via advanced control structures [15], [16] for the accurate reproduction of motion patterns is considered future work, which will enable the evaluation of more complex schemes for simultaneous position and compliance control for safe human-robot interaction.

REFERENCES

[1] G. A. Bekey, "Robotics: State of the Art and Future Challanges," Imperial College Press, 2008.
[2] J. Wang, "A survey on the structures of current mobile humanoid robots", in Proc. of *IEEE Asia Pacific Conference on Circuits and Systems* (APCCAS), 30 Nov. - 3 Dec., 2008, Macao.
[3] H. Inoue "Whither Robotics: Key Issues, Approaches and Applications", IROS'96, Osaka, Japan, 1996, p. 9–14.
[4] R. Drake, "Gray's Anatomy for Students", Third Edition, Elsevier, 2015.
[5] G. Andrikopoulos, G. Nikolakopoulos, and S. Manesis, "A Survey on applications of Pneumatic Artificial Muscles," in *Mediterranean Conference on Control and Automation (MED)*, 2011, pp. 1439-1446.
[6] C. Borst, C. Ott, T. Wimbock, and B. Brunner, "A humanoid upper body system for two-handed manipulation,"
[7] P. Kormushev, D. N. Nenchev, S. Calinon, and D. G. Caldwell, "Upper-body kinesthetic teaching of a free-standing humanoid robot,", in Proc. of *IEEE International Conference on Robotics and Automation* (ICRA), 9-13 May, 2011, Shanghai.
[8] D. Shin, I. Sardellitti, and O. Khatib., "A hybrid actuation approach for human-friendly robot design," in Proc. of the *2008 IEEE International Conference on Robotics and Automation* (ICRA), 2008.
[9] K. Kawashima, T. Sasaki, T. Miyata, N. Nakamura, M. Sekiguchi, and T. Kagawa, "Development of robot using pneumatic artificial rubber muscles to operate construction machinery," *J. Robotics and Mechatronics*, vol. 16, no. 1, pp. 8–15, 2004.
[10] RoboThespian, Engineered Arts Limited (Penryn, Cornwall, U.K. 2010).
[11] I. Boblan and A. Schulz, "A Humanoid Muscle Robot Torso with Biologically Inspired Construction," *in ISR 2010, 41st International Symposium on Robotics and ROBOTIK 2010*, 6th German Conference on Robotics, Munich, Germany, 2010.
[12] B. Tondu and P. Lopez, "Modeling and control of McKibben artificial muscle robot actuators," *IEEE Control Systems Magazine*, vol. 20, no. 2, pp. 15–38, 2000.
[13] R. Dillmann, "Künstliche Muskeln als optimale", Antriebe, Institut für technische Informatik, Universität Karlsruhe.
[14] G. Andrikopoulos, G. Nikolakopoulos and S. Manesis, "An Experimental Study on Thermodynamic Properties of Pneumatic Artificial Muscles", in *20th Mediterranean Conference on Control and Automation* (MED), 3-6 July 2012, pp. 1334-1340, Barcelona, Spain.
[15] G. Andrikopoulos, G. Nikolakopoulos, and S. Manesis, "Advanced Non-linear PID Based Antagonistic Control for Pneumatic Muscle Actuators", in *IEEE Transactions on Industrial Electronics* (TIE), vol. 61, no. 12, pp. 6926 – 6937, December 2014.
[16] G. Andrikopoulos, G. Nikolakopoulos, and S. Manesis, "Pneumatic Artificial Muscles: A Switching Model Predictive Control Approach", in *Control Engineering Practice* (CEP), Elsevier, vol. 21, no. 12, pp. 1653-1664, December 2013.